Science of the Total Environment 839 (2022) 156326

Contents lists available at ScienceDirect

Science of the Total Environment

journal homepage: www.elsevier.com/locate/scitotenv

Disentangling effects of natural and anthropogenic drivers on forest net ecosystem production

You-Ren Wang [a,b,*], Nina Buchmann [c], Dag O. Hessen [a], Frode Stordal [a], Jan Willem Erisman [b,d], Ane Victoria Vollsnes [a], Tom Andersen [a], Han Dolman [b,e]

[a] Centre for Biogeochemistry in the Anthropocene, University of Oslo, Oslo 0316, Norway
[b] Department of Earth Sciences, Vrije Universiteit Amsterdam, Amsterdam 1081 HV, the Netherlands
[c] Department of Environmental Systems Science, ETH Zurich, Zurich 8092, Switzerland
[d] Institute of Environmental Sciences, Leiden University, Leiden 2311, the Netherlands
[e] Royal Netherlands Institute for Sea Research, Texel 1797 SZ, the Netherlands

HIGHLIGHTS

- Impacts of environmental drivers on forest CO_2 fluxes are often mixed.
- We analyzed 231 site-year forest data and 7 natural and anthropogenic driver data.
- We disentangled driver impacts on CO_2 fluxes by GAM regression analysis.
- Thresholds of S and N deposition for substantial impact on NEP were determined.
- We developed novel empirical models for estimating forest net CO_2 fluxes.

GRAPHICAL ABSTRACT

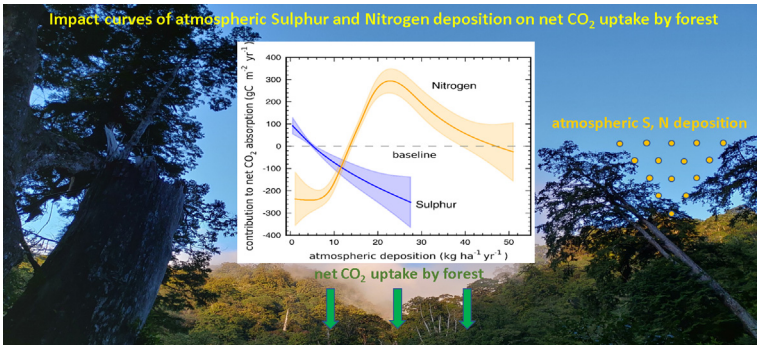

ARTICLE INFO

Editor: Manuel Esteban Lucas-Borja

Keywords:
Forest carbon uptake
NEE
GPP
RECO
Empirical biogeochemical models
GAM

ABSTRACT

Net Ecosystem Production (NEP) of forests is the net carbon dioxide (CO_2) fluxes between land and the atmosphere due to forests' biogeochemical processes. NEP varies with natural drivers such as precipitation, air temperature, solar radiation, plant functional type (PFT), and soil texture, which affect the gross primary production and ecosystem respiration, and thus the net C sequestration. It is also known that deposition of sulphur and nitrogen influences NEP in forest ecosystems. These drivers' respective, unique effects on NEP, however, are often difficult to be individually identified by conventional bivariate analysis. Here we show that by analyzing 22 forest sites with 231 site-year data acquired from FLUXNET database across Europe for the years 2000–2014, the individual, unique effects of these drivers on annual forest CO_2 fluxes can be disentangled using Generalized Additive Models (GAM) for nonlinear regression analysis. We show that S and N deposition have substantial impacts on NEP, where S deposition above 5 kg S ha^{-1} yr^{-1} can significantly reduce NEP, and N deposition around 22 kg N ha^{-1} yr^{-1} has the highest positive effect on NEP. Our results suggest that air quality management of S and N is crucial for maintaining healthy biogeochemical functions of forests to mitigate climate change. Furthermore, the empirical models we developed for estimating NEP of forests can serve as a forest management tool in the context of climate change mitigation. Potential applications include the assessment of forest carbon fluxes in the REDD+ framework of the UNFCCC.

* Corresponding author at: Centre for Biogeochemistry in Anthropocene, University of Oslo, Oslo 0316, Norway.
E-mail address: y.r.wang@ibv.uio.no (Y.-R. Wang).

http://dx.doi.org/10.1016/j.scitotenv.2022.156326
Received 11 March 2022; Received in revised form 6 May 2022; Accepted 25 May 2022
Available online 30 May 2022

1. Introduction

The large biogeochemical sinks of atmospheric CO_2 are formed by NEP of lands and oceans. With the uncertainty included, the terrestrial CO_2 sink globally sequestered on average 3.4 ± 0.9 GtC yr^{-1} over 2010–2019, which offsets fossil CO_2 emissions by 35%, making it a greater carbon sink than the ocean, which is estimated to remove 26% of fossil-fuel-derived CO_2 (Friedlingstein et al., 2020). Further, it has been revealed that the terrestrial CO_2 sink strongly depends on forested areas (Luyssaert et al., 2008; Schulze, 2006), and that forests store some 50%–65% of terrestrial organic carbon, which constitutes half of the global terrestrial productivity (Reichstein and Carvalhais, 2019).

The drivers of NEP analyzed in this study have the potential to impact forest C fluxes in several ways. Deposition of acidifying compounds such as sulphur (S) and nitrogen (N), where N has oxidized and reduced form, may play different roles in acidification and act as key plant nutrients as well (Ciais et al., 2008; Forde and Clarkson, 1999; Fowler, 1992; Galloway, 1995; Johnson, 1984). N is required for tree growth, through which carbon is captured from the atmosphere and stored as biomass. On the other hand, S and N deposition with very high amounts can cause soil acidification (Stevens et al., 2009) and nutrient cation leaching (De Vries and Breeuwsma, 1987), impairing ecosystem health. That ultimately results in the mortality of tissues/trees (Dietze and Moorcroft, 2011), which releases C to the atmosphere through heterotrophic respiration (Anderegg et al., 2016).

However, natural drivers such as precipitation (Gholz et al., 1990), temperature (Lindroth et al., 1998), and solar radiation (Durand et al., 2021; Ruimy et al., 1995) are also primary controls of forest productivity, in addition to the forests' PFT (Welp et al., 2007) and the soil texture (Dilustro et al., 2005). Therefore, understanding the individual effects of environmental drivers that impact the forest CO_2 exchange with the atmosphere is desirable for assessing local and global C cycling in biogeochemistry and thus the effects on climate change (Schulze et al., 2019).

It has been reported that CO_2 fluxes respond in nonlinear fashion to a number of environmental drivers (Flechard et al., 2020a; Flechard et al., 2020b). Such nonlinear feature can be shown by conventional bivariate analysis, for example, the loess regression (Jacoby, 2000), which depicts the simple relation between one response variable and one explanatory variable at a time, without referencing to other explanatory variables that act simultaneously on the response variable. Therefore, the simple relation between two variables in bivariate analysis represents mixing effects of environmental drivers on CO_2 fluxes.

In this work, in order to reveal the unique, unmixed contribution of an environmental driver, we utilize GAM to disentangle and nonlinearly model the dependence of CO_2 fluxes on the seven drivers. As the importance of applications of various biogeochemical models that estimate land CO_2 uptake is increasing in recent years (Ciais et al., 2019; Ciais et al., 2021; Flechard et al., 2020b; Papale et al., 2015), our study, in parallel with those efforts, developed novel empirical models that use seven environmental drivers as input for quick CO_2 flux assessments of forest sites.

2. Material and methods

The data that constitute the basis of this work are composed of micrometeorologically measured annual forest CO_2 fluxes and meteorological data from the synthesized FLUXNET2015 dataset (Baldocchi et al., 2001; Pastorello et al., 2017; Pastorello et al., 2020) in the FLUXNET database (FLUXNET, accessed 24 April 2020), and the modelled annual deposition data of oxidized sulphur (SOX), oxidized nitrogen (OXN), and reduced nitrogen (RDN) from EMEP MSC-W database (MET, accessed 20 November 2019) on a 0.1° × 0.1° grid in Europe (Fig. 1). Soil texture data and PFT data are also used.

2.1. FLUXNET

FLUXNET is a global network of micrometeorological tower sites that use eddy covariance methods to measure the exchanges of carbon dioxide, water vapor, and energy between terrestrial ecosystems and the atmosphere. The eddy covariance method is currently the standard method used by biometeorologists to measure fluxes of trace gases between ecosystems and atmosphere.

Fluxes are measured by computing the covariance between the vertical wind speed and target scalar mixing ratios at each individual site, assuming storage within the canopy and advection fluxes to be negligible. Net ecosystem CO_2 fluxes are measured at FLUXNET tower locations, which are further partitioned empirically into Gross Primary Productivity (GPP), representing the photosynthetically assimilated C flux going into the forest, and ECOsystem Respiration (RECO), representing the C flux going out of the forest. Both of GPP and RECO are defined as positive quantities.

NEE (Papale et al., 2006; Reichstein et al., 2005) is the measured net CO_2 exchange of an ecosystem with the atmosphere, equivalent to RECO subtracted by GPP:

$$NEE = RECO - GPP \quad (1)$$

where RECO is the sum of autotrophic respiration and heterotrophic respiration of the ecosystem. Summed up on an annual basis, NEP is defined as -NEE. Thus, without taking additional carbon imports or exports (e.g. liming or harvest) into consideration, NEP is an indicator for identifying if a forest site is an annual CO_2 sink (positive) or source (negative).

2.1.1. FLUXNET2015 dataset

As of September 2020, the FLUXNET2015 is the latest synthesis dataset released by the FLUXNET collaboration, incorporating data collected at sites from multiple regional flux networks up to year 2014. The FLUXNET2015 Dataset includes several improvements to the data quality control protocols and the data processing pipeline over the previous versions of FLUXNET Datasets.

The data processing pipeline for the FLUXNET2015 Dataset was developed in a collaboration between personnel from the European Ecosystem Fluxes Database, ICOS Ecosystem Thematic Centre (ICOS-ETC) and the AmeriFlux Management Project (AMP). It adapts code developed by the community, integrating with code developed by the teams into a consistent and uniform data processing pipeline. The starting point for the data processing is half-hourly data collected and processed at FLUXNET sites. The pipeline procedure, OneFlux, generates uniform and high-quality derived data products suitable for studies requiring intercomparability of data from multiple sites. The harmonization and data quality control activities are particularly important for the FLUXNET2015 Database.

2.1.2. FLUXNET2015 data acquisition

The FULLSET Data Product of the FLUXNET2015 Release are acquired for this study (including both Tier1 and Tier2), and the dataset of the standard yearly (YY) temporal aggregation are adopted. Six variables in the datasets are used in this study, including NEE_VUT_REF (for NEP), RECO_NT_VUT_REF (for RECO), GPP_NT_VUT_REF (for GPP), SW_IN_F_MDS (for SW radiation), P_F (for precipitation), and TA_F (for air temperature). These datasets were made by the FLUXNET collaboration, as summarized in Table 1.

2.1.3. Data selection criteria and the final dataset

Four levels of data selection were used in this study for the selection of FLUXNET2015 forest site-year data. For the period 2000–2014 in Europe, there are totally 32 forest sites with 318 site-years in the FLUXNET2015 yearly temporal aggregation database. In each site-year data, the yearly Net Ecosystem Exchange (NEE_VUT_REF) flux is associated with a quality flag (NEE_VUT_REF_QC). The first-level selection criterion is that for these 318 site-year data, only those with a quality flag greater than 0.75 are considered high quality and selected. 31 sites with 266 site-years pass this first-level selection.

The second-level selection criterion is that the number of site-years that passed the first-level selection of any site should be more than three. The purpose is to include only those sites with sufficient length in order to

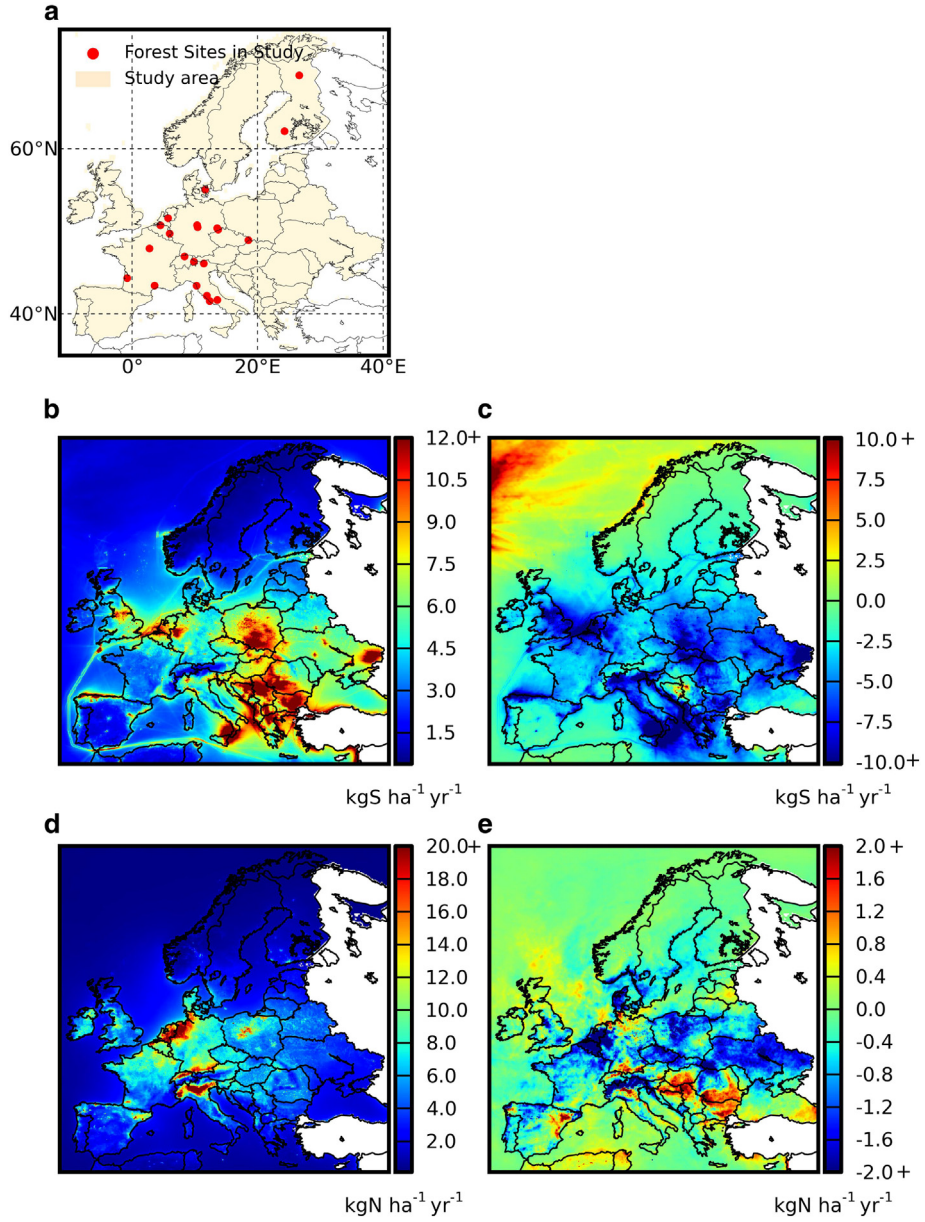

Fig. 1. Geographical distributions of data used in this work. (a) Locations of the 22 FLUXNET forest sites. (b) 2000–2014 averaged S deposition. (c) S deposition difference between year 2014 and 2000 (2014 deposition subtracted by 2000 deposition). (d) 2000–2014 averaged total N deposition. (e) N deposition difference between year 2014 and 2000. (c) and (e) indicate that S and N depositions have considerably decreased during the 15-yr period in most regions in Europe, however, there are areas where S/N deposition increased instead. S deposition from the 2014–2015 volcanic eruption of Bárðarbunga in Iceland is visible in the upper left corner of (c).

preserve the trend of the site. 23 sites with 250 site-years survive the second-level selection.

The third-level selection criterion is that the quality flag (SW_IN_F_MDS_QC) for Shortwave radiation must be greater than 0.75 to ensure high quality. 7 site-years did not pass this criterion. And the final selection criterion filtered out outliers with exceptionally high NEP compared to the rest in the dataset. 22 sites with 231 site-years survived all the four-level criteria.

The four-stage selection criteria were designed to exclude data with insufficient quality and length, while preserving the maximum possible site-years for analysis to minimize selection bias.

As the result, in-situ measured data analyzed in this study include 22 FLUXNET2015 forest sites (Table S1, Fig. 1a) having a total of 231 site-year annual averaged EC-derived CO_2 fluxes of NEE, GPP and RECO from the latest database release (Table S2), as well as meteorological data of annual precipitation, air temperature, and incoming shortwave solar radiation measured in the period 2000–2014 at the site locations across Europe.

Soil texture data of sites CH-Dav, DE-Lnf, DE-Obe, IT-Cpz, and IT-Ro1 were provided by the PIs of those five sites. Soil texture data of the rest of 17 sites were acquired from Table S4 in published literature (Flechard et al., 2020a).

In this study, loamy clay and silty clay are classified as clay soil; clayey loam and silty loam are classified as loam soil; clayey sand, loamy sand, and pure sand are classified as sand soil; sandy silt is classified as silt soil.

Plant functional types of the sites were also acquired from FLUXNET2015. PFT of the final selected 231 site-years are: Evergreen Needleleaf Forest (10 sites, 112 site-years), Deciduous Broadleaf Forest (7 sites, 62 site-years), Mixed Forest (3 sites, 37 site-years), and Evergreen Broadleaf Forest (2 sites, 20 site-years).

All the seven environmental driver data of the 231 site-years are summarized in Table S3.

Table 1
Data acquired from the FLUXET2015 release.

Variable in dataset	Common name	Procedure (by FLUXNET collaboration)
NEE_VUT_REF	Net ecosystem exchange	Data were produced using the Variable u* Threshold (VUT) of each year. 40 different NEE estimations were calculated by filtering the original NEE data with 40 different Ustar thresholds. Then the one with higher Model Efficiency sum was selected and released as the reference NEE (NEE_VUT_REF). By definition, NEP shown in this study is equal to negative NEE_VUT_REF.
RECO_NT_VUT_REF	Ecosystem respiration	Data were produced from NEE using the Nighttime Partitioning Method (Reichstein et al., 2005). The nighttime data were used to parameterize a respiration model that was then applied to the whole dataset to estimate RECO. The reference RECO (RECO_NT_VUT_REF) was made and released in the same way as NEE_VUT_REF.
GPP_NT_VUT_REF	Gross primary production	Data were produced from NEE using the Nighttime Partitioning Method. The reference GPP (GPP_NT_VUT_REF) was made and released in the same way as NEE. It is noteworthy that the u* thresholds that result in the REF versions of NEE, RECO, and GPP are not necessarily the same for these three carbon fluxes. Therefore, unlike the relation described in Eq. (1), for the data used this analysis, GPP subtracted by RECO is close, but not equal to NEP.
SW_IN_F_MDS	Shortwave radiation	Data were incoming and gap-filled using MDS (negative values set to zero, e.g., negative values from instrumentation noise). Yearly data are the average from daily data, which are the average from half-hourly data.
P_F	Precipitation	Data were the annual sum of the daily precipitation, consolidated from P and P_ERA, where P were the measured precipitation, and P_ERA were downscaled from ERA, linearly regressed using measured-only site data.
TA_F	Air temperature	Data were averaged from daily air temperature, consolidated from TA_F_MDS and TA_ERA, where TA_F_MDS were gapfilled using MDS method, and TA_ERA were downscaled from ERA, linearly regressed using measured-only site data.

2.2. EMEP MSC-W

Modelled data acquired for this study include annual 0.1° × 0.1° gridded SOX, OXN and RDN deposition across Europe from the EMEP MSC-W (Fagerli et al., 2019; Simpson et al., 2012; Simpson et al., 2006) database of MET Norway. EMEP (European Monitoring and Evaluation Programme) is a scientifically based and policy driven programme under the Convention on Long-range Transboundary Air Pollution (CLRTAP) for international co-operation to solve transboundary air pollution problems. With the incorporation of emission data and meteorological conditions, the EMEP MSC-W has been performing chemical transport model calculations for more than 30 years, and acts as one of the key tools for European air pollution policy assessments.

2.2.1. Modelled S and N deposition dataset

In the database of EMEP MSC-W modelled air concentrations and depositions, S and N deposition gridded data are available for Europe from year 2000 onwards with a grid resolution of 0.1° × 0.1° (MET, accessed 20.Nov.2019). For the period 2000–2014, we acquired yearly S and N deposition Type2 datasets that EMEP recalculated in 2019, in accordance with the data availability of FLUXNET2015. The three types of gridded S and N deposition data used in this study include:

SOX: Total deposition of dry and wet oxidized sulphur (DDEP_SOX_m2Grid + WDEP_SOX),

OXN: Total deposition of dry and wet oxidized nitrogen (DDEP_OXN_m2Grid + WDEP_OXN),

RDN: Total deposition of dry and wet reduced nitrogen (DDEP_RDN_m2Grid + WDEP_RDN).

Total deposition of SOX is the sum of the dry and wet deposition of SO_2 and SO_4^{2-}. By far the major source of SOX is the combustion of S-containing coal and oil at power plants and in industrial boilers. Burning of S-containing fuels in motor vehicles and marine engines, smelting of metals in industry as well as volcanic eruptions also produce SOX. The paths of vessels burning heavy oil and the near-continuous emissions from Strombolian eruptions are also visible in the marine regions (Fig. 1b).

In the EMEP MSC-W model, the dry and wet deposition that forms the total deposition of OXN mainly includes components of NO_2, $NO_3^-{}_{PM\_fine}$, $NO_3^-{}_{PM\_coarse}$, and HNO_3. NO_2 is produced primarily through rapid reaction of ozone with NO, the main emissions from combustion of fossil fuels by traffic, transport, industry and energy production (Fowler et al., 2009). NO_3^- in particles is formed by reaction of HNO_3 with NH_3 in the air.

RDN deposition in the model is composed of wet and dry deposition of NH_3 and $NH_4^+{}_{PM\_fine}$. The anthropogenic sources of NH_3 are agricultural activities and animal housing and grazing operations followed by biomass burning and to a lesser extent, fossil fuel combustion. NH_4^+ is formed when NH_3 reacts with HNO_3, HCI and/or H_2SO_4 in the atmosphere to form particulate matter. In this study, OXN and RDN depositions were summed up to compose the driver of total reactive N deposition (Fig. 1c).

2.2.2. S and N deposition data acquisition

The yearly SOX, OXN, and RDN depositions corresponding to the 231 site-year FLUXNET data used in this analysis were extracted from the EMEP datasets based on the site years and site coordinates. It was done by identifying the 22 grid points in the EMEP 0.1° × 0.1° grid that are closest to the 22 FLUXNET site locations first. The S and N depositions of those 22 grid points were then regarded as the depositions at the corresponding 22 FLUXNET sites of the respective years. The SOX, OXN, and RDN depositions corresponding to the FLUXNET 231 site-year data were therefore obtained.

The average bias of the modelled S wet depositions for 2017 are −27% compared to measurements (Gauss et al., 2019) and somewhat lower for N wet depositions. Due to the limited number of dry deposition measurements available, a quantification of bias in the dry deposition is more difficult. A limited comparison to dry (and wet) deposition of nitrogen suggests that the EMEP MSC-W model is capturing the main deposition processes in a reasonable way. A comparison of annual EMEP model results and EMEP measurements for gas, particle and deposition of N across Europe showed that the correlation coefficients vary between 0.62 and 0.87 (Simpson et al., 2006).

2.3. Generalized additive models

In this study, forest carbon fluxes NEP, GPP, and RECO are the responsive variables, and are modelled by the seven environmental explanatory variables using GAM package 'mgcv' implemented in R (Wood, 2022a; Wood, 2022b; Wood, 2017). GAM is a powerful statistical tool capable of fitting models without the need to specify the parametric relations between the responsive and explanatory variables (Hastie and Tibshirani, 1990).

The GAM regression result is expressed as a sum of smooth functions of each variable, such that each explanatory variable has an additive effect on the resultant responsive variable. A GAM model can be expressed as:

$$Y = c + f_1(x_1) + f_2(x_2) + \cdots + f_n(x_n) + \varepsilon \quad (2)$$

where Y is the responsive variable, $f(x)$ is the modelled smooth function of an explanatory variable x, c is the modelled constant term (intercept) of the model, and ε is the uncertainty of the regression. C can be interpreted as the baseline value of the model, to which the varying contributions of explanatory variables add their values and result in Y.

Smooth non-parametric functions were used for fitting the relationship between the responsive variable and explanatory variables. Cubic regression spline basis functions with shrinkage were adopted in this work. Generalized cross-validation was selected such that the number of knots for modelling is automatically determined for balancing simplicity against explanatory power. Categorical data, such as soil texture and PFT in this study, were treated as linear terms without smoothing in GAM (Buja et al., 1989). Goodness-of-fit and overfitting were balanced via minimizing the average squared difference between the original data and the values predicted by the smooth functions (Johnston et al., 2019; Wood, 2004).

The contribution of each explanatory variable is therefore revealed by examining each function of the individual variable (Yee and Mitchell, 1991).

GAM regression analysis was employed to find out how each of the seven drivers, from their own unique contribution, can affect CO_2 fluxes at their different level of strengths. Once the contributions of drivers are disentangled, GAM is not further used. And the unique, unmixed contribution of each driver can then be added up to construct predicted CO_2 fluxes. NEP-predicting, GPP-predicting, and RECO-predicting models can thus be formed, applicable to forests that have the seven environmental drivers being within the ranges of the 231 site-years in this study.

2.4. GAM versus bivariate analysis

Before performing GAM regression analysis, we applied bivariate analysis for testing the simple relation between NEP and the seven environmental drivers respectively (Fig. S1). The bivariate analysis was done by applying nonlinear Loess regression on each of the scatter plots of NEP and the environmental drivers, respectively. It is noteworthy that in the bivariate analysis, the changes of NEP cannot be solely attributed to the changes of the single environmental driver being tested, since all other drivers are also changing and affecting CO_2 fluxes simultaneously as the driver changes. This causes the simple relations between NEP and the drivers, as shown by the curves in Fig. S1, to be spurious "dependence". Such dependence has no additive feature to construct a NEP-predicting model, and therefore is not further used in this study.

GAM analysis, however, analyzes NEP and the seven drivers altogether in one run, and is able to disentangle the complex and reveal the individual, unmixed contribution of each single driver to forest C fluxes. The additive feature allows to construct an NEP-predicting model by adding up the disentangled driver contributions to NEP.

3. Results and discussion

3.1. GAM regression analysis

The GAM regression analysis was performed for NEP (Fig. 2), GPP (Fig. 3), and RECO (Fig. 4). The proportions of variance of NEP, GPP, RECO fluxes explained by the regression are 57.2%, 84.3%, and 55.4%, respectively. Each graph shows the effects of an individual driver on the CO_2 fluxes at all levels of the driver' strengths. A positive value indicates that the contribution to the flux from the driver at that level of strength is to increase the flux from the modelled baseline level, and vice versa. Below we summarize the GAM regression analysis results of NEP, GPP, and RECO, with respect to each of the seven environmental drivers.

3.2. Concurvity check

Concurvity, the analogue of multicollinearity in linear regression, represents the degree to which the smooth functions in the model can be approximated by other smooth functions. Concurvity ranges between 0 and 1, where 0 indicates no concurvity between variables, and 1 occurs when the variables are not distinguishable (Wood, 2017).

Concurvity indicates interference between smooth function, which causes problems in the interpretation of the results when it is too high. Cubic regression spline basis functions for the GAM regression model were adopted, which help reduce concurvity between smooth functions in the model (Buja et al., 1989). While the universal criterion for acceptable concurvity has not been established, concurvity below 0.3 is normally considered low (Johnston et al., 2019). Estimated concurvity values between pairs of the seven drivers in this study are shown in Table 2.

3.3. Disentangled driver effects on forest carbon fluxes

3.3.1. S deposition

The contribution to NEP decreases monotonically as S increases (Fig. 2a). At lower levels, S deposition has positive contribution to NEP relative to the baseline level, and it turns negative after around 5 kg S ha^{-1} yr^{-1}, showing a threshold of S response. It is interesting to note that GPP also had a negative response to increasing S deposition, whereas RECO did not, indicating that the response was due to how plant carbon fixation responded to the S deposition.

S deposition is among the primary sources of acid rain, which has been shown to cause widespread damage to vegetation and can deplete nutrients in soils (Johnson, 1984). As a consequence, vegetation becomes more vulnerable to environmental stress (DeHayes et al., 1999). Acidified soils and surface waters cause cation depletion and result in a decline in vegetation growth or even mortality (Schulze et al., 1989). The critical loads, defined as 'the highest load that will not cause chemical changes leading to long-term harmful effects on most sensitive ecological systems' (Nilsson, 1988), was reported for S deposition to be 2–4 kg S ha^{-1} yr^{-1} for Europe (Nilsson, 1988). In addition, the CLRTAP of the United Nations Economic Commission for Europe (UNECE) has also developed a database for European critical loads (Hettelingh et al., 2017). The current critical loads for acidification vary greatly across Europe, from less than 3.2 to above 24 kg S ha^{-1} yr^{-1}. Moreover, some countries had started to report on critical levels for biodiversity, but that work has to be increased in the future.

In the view of terrestrial CO_2 exchange, this study provides the impact curve of S in a wide range, and further reveals that S is a major suppressor of NEP of the forest ecosystem by reducing GPP as it increases (Fig. 3a).

3.3.2. N deposition

Studies have demonstrated that N deposition can stimulate plant growth and increase carbon uptake (Pregitzer et al., 2008; Reay et al., 2008; Thomas et al., 2010), and can even be the dominant driver of carbon sequestration in forest ecosystems (Magnani et al., 2007). The long-term critical load for N was reported to be in the range of 10–20 kg N ha^{-1} yr^{-1} for most forest ecosystems (Dise et al., 2011).

Our work determines an optimal level of N at around 22 kg N ha^{-1} yr^{-1} (Fig. 2b) to have the highest contribution to NEP, above which the contribution to NEP starts to decrease monotonically till the end of the curve. This supports the findings of Flechard et al. (2020a). They reported increased NEP of forests as N deposition increased up to a level of 20–25 kg N ha^{-1} yr^{-1} and a subsequent decrease. The authors cautioned that there could be a cross-correlation with climate, as the sites with the lowest N deposition in their analysis also had low values of mean annual temperature and precipitation. Further, the sites with the highest NEP also had higher mean annual temperature and wetter climate than the sites with lower N deposition. In our current analysis, we have found the same positive effect of increased N deposition rates at low levels even when the effects of mean annual temperature and precipitation have been accounted for separately in the models, supporting the supposition that increasing N deposition up to a level of 22 kg N ha^{-1} yr^{-1} has a positive effect on forest NEP. Flechard et al. (2020a) also found a negative effect of high N deposition on forest NEP. In their analysis, the negative effects could be due to increased N losses as leaching or emissions of NO_x gasses at the highest N deposition sites.

In our study, N deposition below 14 kg N ha^{-1} yr^{-1}, on the other hand, contributes negatively to NEP relative to the baseline level, implying a threshold level of N, below which the forests may encounter N limitation for growth.

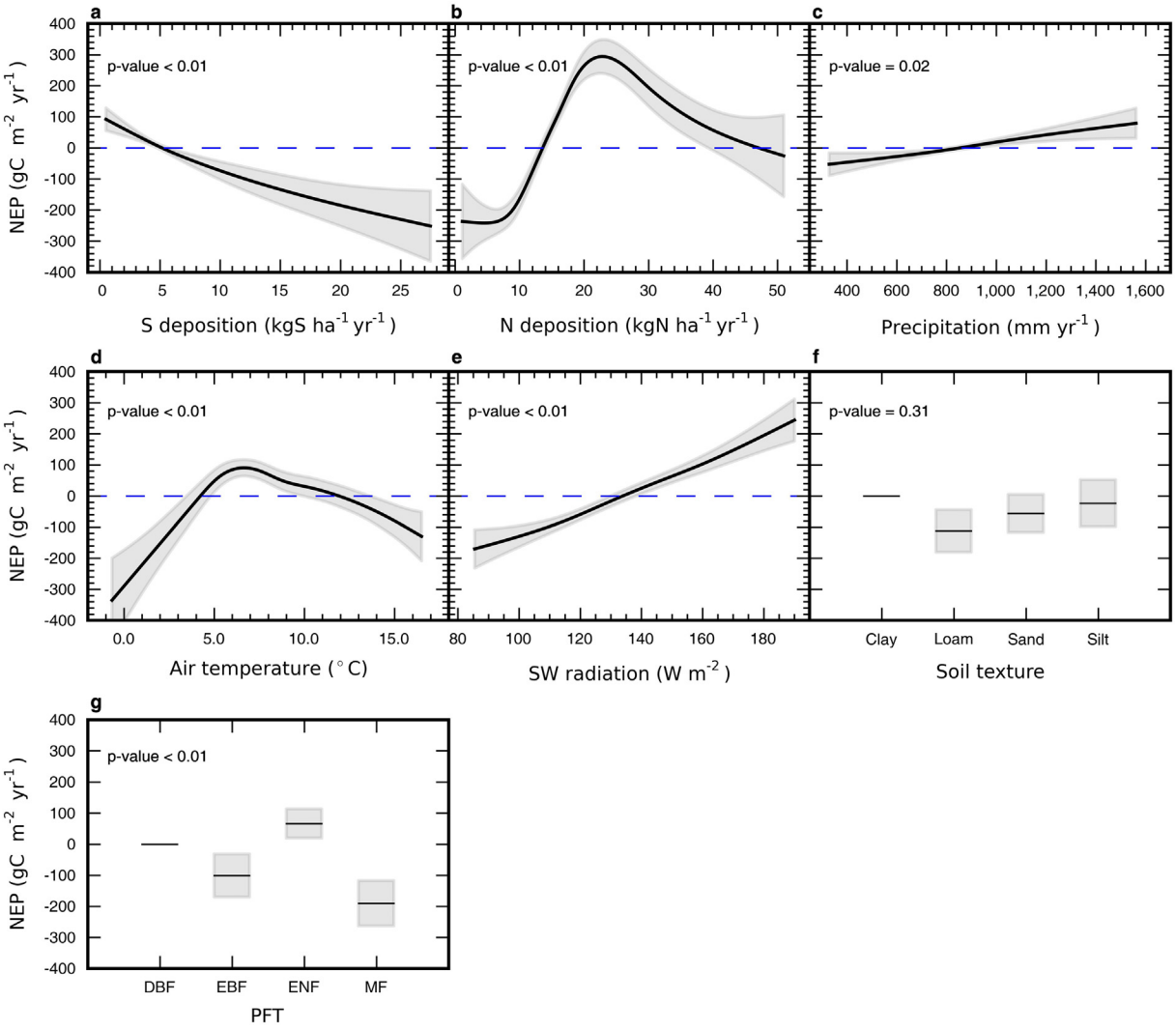

Fig. 2. GAM regression analysis results for NEP partial dependence on the seven environmental drivers at all strength levels. The Y axis shows driver contributions to NEP relative to the modelled baseline. Contributions from (a) S deposition; (b) N deposition; (c) precipitation; (d) air temperature; (e) incoming shortwave radiation; (f) soil texture; and (g) PFT. All the gray bands show 1σ uncertainty. The modelled baseline NEP level is 478.0 gC m^{-2} yr^{-1}. Except for soil texture, the *p*-values of the other six drivers are all below 0.05, showing statistical significance in impacting NEP.

Although N deposition beyond the optimal level appears to still contribute to NEP positively, however, the adverse effects of N at substantially elevated levels should not be underestimated, which include soil acidity (Binkley and Högberg, 2016; Chien et al., 2008) and damage to forest growth (Erisman et al., 2007). Bobbink and Hettelingh, 2011 reviewed and revised the European empirical critical loads for N deposition to forests. Depending on forest type, the critical loads were found to be between 3 and 20 kg N ha^{-1} yr^{-1}. The negative effects underlying the identification of the upper level of critical loads are for instance changes in ground vegetation, mycorrhiza development and fine root growth. Our finding of decreasing forest NEP above 22 kg N ha^{-1} yr^{-1} could also be influenced by such ecological effects.

3.3.3. Precipitation

Precipitation is known to impact CO_2 fluxes of ecosystems (Schwalm et al., 2010), and frequent extreme drought events may erode the health and productivity of ecosystems (Ciais et al., 2005). Fig. 2c indicates that in the regular precipitation range, while the impact of precipitation to RECO is statistically insignificant (Fig. 4c), as precipitation increases, the contribution to GPP significantly increases (Fig. 3c). This results in a linear but relatively weak impact of precipitation on NEP, with the curve intercepting the baseline at around 900 mm yr^{-1}.

3.3.4. Air temperature

Air temperature is documented to affect forest GPP (Ciais et al., 2005; von Buttlar et al., 2018) and soil respiration (Joos et al., 2001). Figs. 3d and 4d show that higher mean annual air temperature causes higher GPP and RECO in general. The resultant effect makes air temperature to form an optimal temperature range between 4 °C and 12 °C with positive contribution on NEP (Fig. 2d) relative to the baseline. The larger the deviation from this optimal temperature range is, either positively or negatively, the larger the decrease in NEP is.

3.3.5. SW radiation

SW radiation is often used in lieu of photosynthetically active radiation (Green et al., 2020). It has been shown that photosynthetic photon fluxes have a curvilinear relation with gross CO_2 fluxes of forests (Ruimy et al., 1995) in experiments in the growing season. Our study reports that NEP increases as mean annual SW radiation increases in the whole range studied (Fig. 2e). Although as SW radiation increases, GPP and RECO do not show monotonic patterns (Figs. 3e and 4e), however, the trends cancel out and result in a strong linear trend in increasing NEP, with the curve intercepting the baseline at around 130 W m^{-2}.

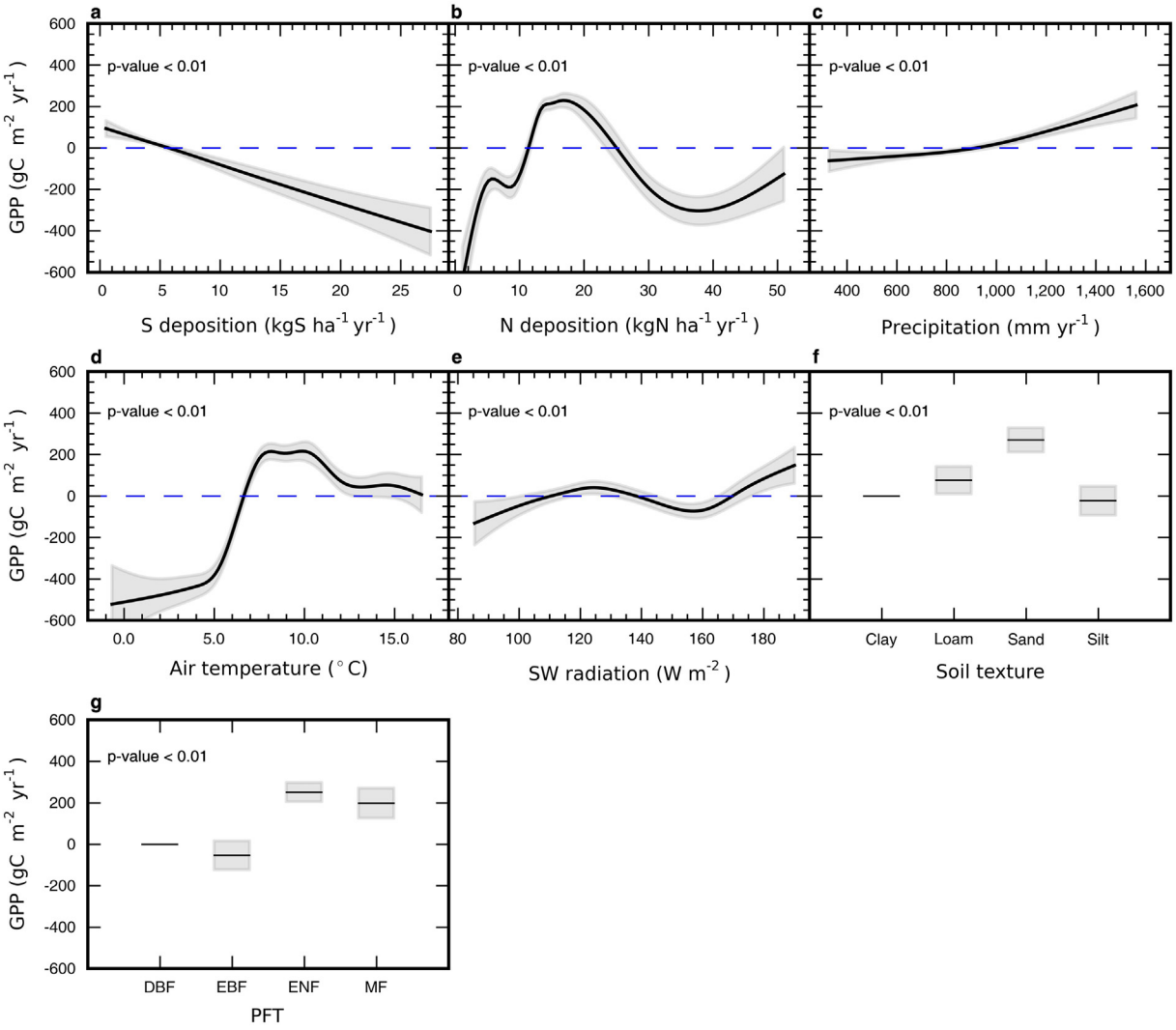

Fig. 3. GAM regression analysis results for GPP partial dependence on the seven environmental drivers at all strength levels. The Y axis shows driver contributions to GPP relative to the modelled baseline. Contributions from (a) S deposition; (b) N deposition; (c) precipitation; (d) air temperature; (e) incoming shortwave radiation; (f) soil texture; and (g) PFT. All the gray bands show 1σ uncertainty. The modelled baseline GPP level is 1243.3 gC m^{-2} yr^{-1}. The *p*-values of the seven drivers are all below 0.05, showing statistical significance in impacting GPP.

The sites studied are located at a range of latitudes from 42 to 67°N, making the results valid for a large area with diverse local conditions. The latitude differences result in great variability in some biologically important factors, the summer daylength (midnight sun at the northernmost site), the summer mean temperature and length of the growing season. The latter two are also affected by the altitudes, varying from lowland to alpine areas. Thus, the effects of these factors are captured by the two environmental drivers mean annual air temperature and mean annual SW radiation in the current GAM analyses.

3.3.6. Soil texture

Soil texture is a categorical driver, and the impact is not a smooth curve but discrete values. The first category is always set to zero in GAM analysis, and the remaining categories show their contribution to NEP relative to it. The result indicates that the *p*-value of the impact of soil texture is 0.31, and therefore is an insignificant driver in this study. On the other hand, both GPP and RECO differed significantly depending on soil type. Soil type will have great impact on water holding capacity, cation exchange capacity and acidity, thus affecting GPP through the plants' access to water and minerals and RECO through the activity of roots and other soil living organisms.

3.3.7. PFT

Plant functional types are system that classifies plants according to their physical, phylogenetic and phenological characteristics for the development of vegetation modelling. PFT is also a categorical driver, and the result shows that among the four types, forests being ENF have the highest positive contribution to NEP. Since evergreen trees may have carbon capturing activity during periods when the deciduous trees are without leaves, this is not so surprising.

3.4. GAM modelling for individual PFT

Fig. 2 presents GAM modelling results for NEP with all the 231 site-year data synthetically analyzed. However, GAM modelling for individual PFTs is also of interest. In Fig. 5, the NEP models for ENF (112 site-years) and for DBF (62 site-years) respectively are superimposed with the model in Fig. 2 for comparison. Note that MF (37 site-years) and EBF (20 site-years) do not have sufficient number of site-years to construct their models.

The three curves from the different PFT groups demonstrate that even with only partial data modelled, the driver impact curves still preserve the patterns of the model using the complete dataset, suggesting that GAM modelling in this work provides robust results.

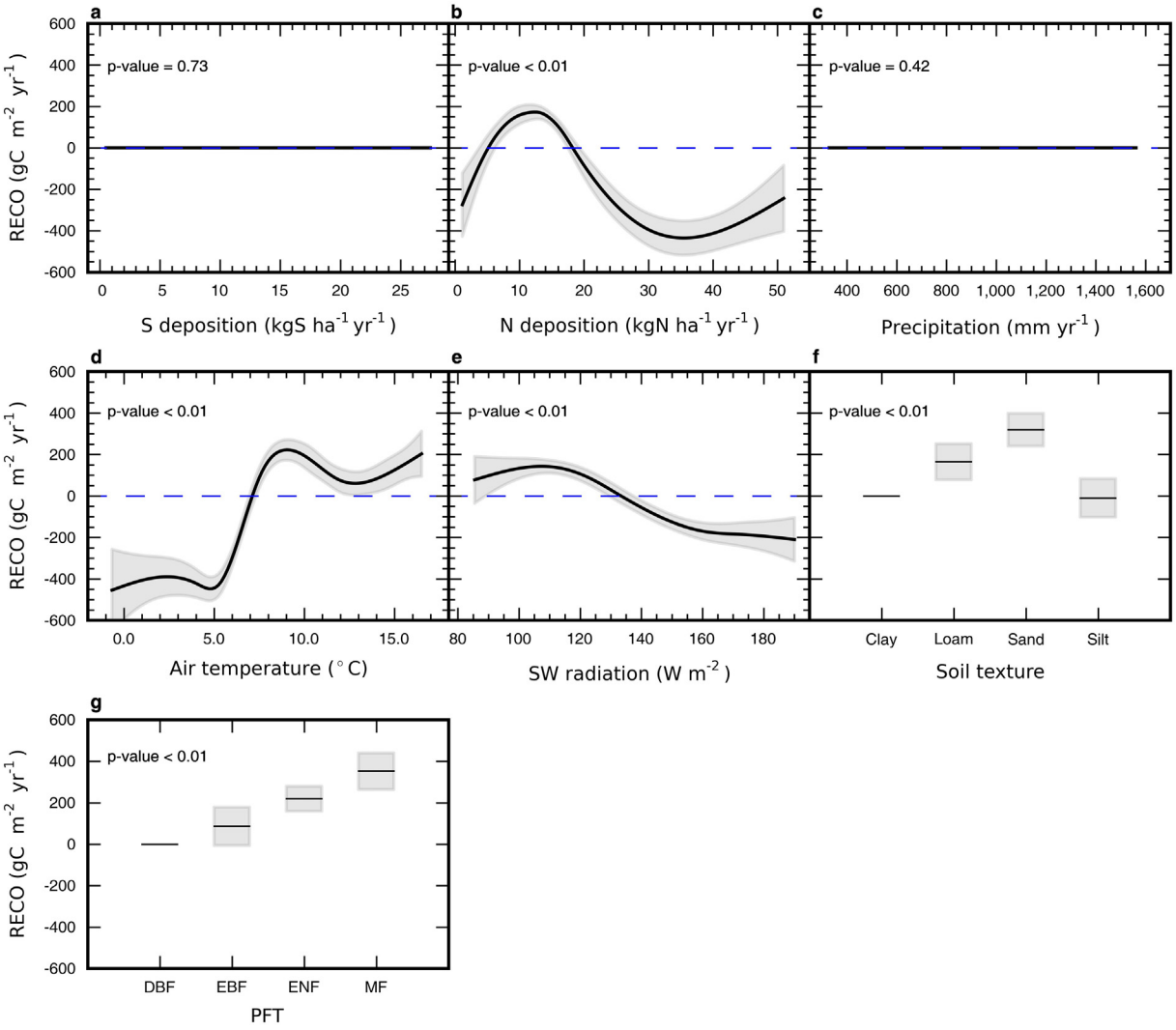

Fig. 4. GAM regression analysis results for RECO partial dependence on the seven environmental drivers at all strength levels. The Y axis shows driver contributions to RECO relative to the modelled baseline. Contributions from (a) S deposition; (b) N deposition; (c) precipitation; (d) air temperature; (e) incoming shortwave radiation; (f) soil texture; and (g) PFT. All the gray bands show 1σ uncertainty. The modelled baseline RECO level is 749.5 gC m^{-2} yr^{-1}. Except for S deposition and precipitation, the *p*-values of the other five drivers are all below 0.05, showing statistical significance in impacting RECO.

3.5. NEP reconstruction and model application

After obtaining the driver response curves, NEP can be reconstructed from the driver values using Eq. (2), as illustrated in Fig. 6. For selected one site-year per PFT, Table 3 summarizes the modelled NEP contribution of each driver, the sum of them, and the difference between modelled and actual NEP. Table S7 further presents these values averaged over all the available years for each of the 22 sites in study.

Based on the 231 site-year data, we developed NEP-predicting (Fig. 2), GPP-predicting (Fig. 3), and RECO-predicting (Fig. 4) models, which can be used to estimate CO_2-fluxes of forests using the method illustrated in Fig. 6, as long as the seven environmental drivers of the forests are within the ranges of the 231 site-years in this study. While it is not practical to include all environmental factors in the model, we believe our empirical models can reasonably capture the biogeochemical CO_2 fluxes of forests based on seven natural and anthropogenic drivers.

Table 2
Estimated concurvity between pairs of the seven drivers.

Concurvity	S deposition	N deposition	Precipitation	Temperature	SW radiation	PFT	Soil texture
S deposition	1.00	0.20	0.06	0.19	0.13	0.00	0.00
N deposition		1.00	0.12	0.29	0.27	0.00	0.00
Precipitation			1.00	0.07	0.10	0.00	0.00
Temperature				1.00	0.25	0.00	0.00
SW radiation					1.00	0.00	0.00
PFT						1.00	0.00
Soil texture							1.00

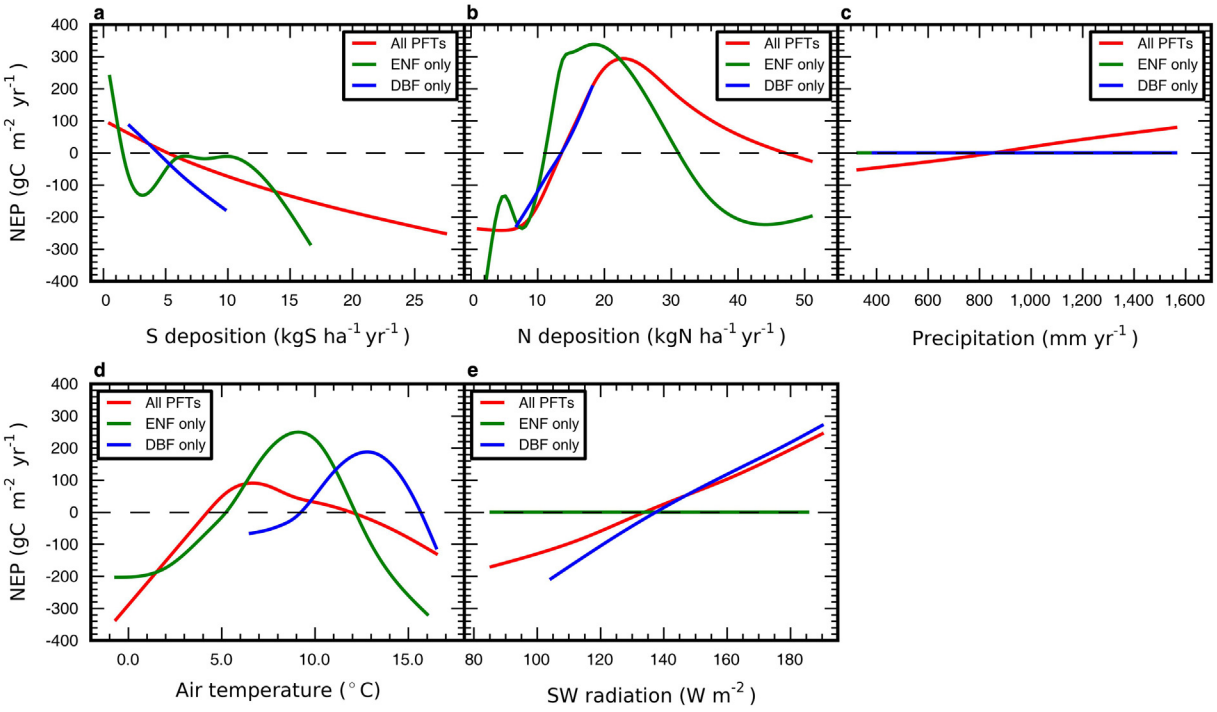

Fig. 5. GAM regression analysis results for NEP by using all the PFTs, ENF only, and DBF only. Contributions from (a) S deposition; (b) N deposition; (c) precipitation; (d) air temperature; and (e) incoming shortwave radiation.

3.6. GAM analysis with natural drivers only

It is interesting to examine whether the five natural drivers in study are already sufficient to explain NEP in the 231 site-years. GAM regression analysis was therefore performed for NEP with only the five natural drivers as the explanatory variables (Fig. S2).

It is seen that the contribution curves (levels) of the five drivers have similar patterns as those in Fig. 2, which were obtained using all the seven drivers. This indicates that the NEP dependence on drivers do not change dramatically even with a few explanatory drivers removed.

However, as discussed in Section 3.1, with S and N depositions included, the proportion of variance explained by GAM regression is 57.2% for NEP. Without S and N depositions, GAM regression here reveals that the proportion is reduced to 48.7%. This demonstrates that including S and N depositions as explanatory variables in addition to natural drivers does increase the overall explanatory power of the drivers. Therefore, S and N depositions do play roles in affecting forest NEP, which are unexplainable by the natural drivers in study.

4. Conclusions

Our study reveals that while S deposition shows a clear impact to reduce NEP at elevated levels, the impact of excessively high N deposition is less clear. To prevent the loss of CO_2 uptake and to improve air quality and biodiversity (Aherne and Posch, 2013), it is important that actions be taken to further control S and N depositions. Potential mitigation measures include, but are not limited to, the review of the policy for coal-fired power plants (Harrison, 2017), vehicles using fossil fuels, fertilizer use, and agricultural production, to echo the appeal in the Paris Agreement that "Parties should take action to conserve and enhance, as appropriate, sinks and reservoirs of greenhouse gases as referred to in Article 4, paragraph 1(d), of the Convention, including forests" (UNFCCC, 2015).

There have been various attempts on estimating forest CO_2 fluxes in recent years, globally or regionally (Blujdea et al., 2021; Grassi et al., 2018; Ma et al., 2021). It is particularly noticeable that in those forest CO_2-predicting models, including the bookkeeping, DGVM, Ecosystem Demography, CBM, and EFISCEN models, the effect of S deposition is not considered. This may cause an underestimation of the detrimental effects of air pollution and thus an overestimation of forest NEP, depending on the level of S deposition.

In parallel with these recent attempts, the empirical NEP, GPP and RECO models that we developed in this work provide a convenient way for estimating forest CO_2 fluxes with seven drivers considered. Potential applications of these models include the assessment of carbon fluxes for REDD+. REDD+ is a framework created by the United Nations Framework Convention on Climate Change (UNFCCC, accessed 24 February 2022) Conference of the Parties (COP) to guide activities in the forest sector that Reduces Emissions from Deforestation and forest Degradation, as well as the sustainable management of forests and the conservation and enhancement of forest carbon stocks in developing countries (UNFCCC, accessed 24. Feb. 2022). Central to the REDD+ framework is the forest carbon accounting, which requires a monitoring, reporting and verifying (MRV) system that tracks changes in forest carbon stocks (Gupta et al., 2012). Therefore, establishing functional MRV systems is one of the major goals of the so called 'REDD Readiness' (Fry, 2011). Failure to account for net ecosystem carbon balance in REDD+ activities will lead to large uncertainty in estimating carbon emissions by forested landscapes (Vargas et al., 2013).

As the current MRV methodologies mainly rely on forest inventory (Maniatis and Mollicone, 2010; Ochieng et al., 2016) and remote sensing (Mitchell et al., 2017; Sirro et al., 2018) approaches, which primarily determine aboveground net primary production, there is a lack of information of carbon losses due to ecosystem respiration from soil and belowground carbon (Vargas et al., 2013). Our empirical models for NEP, GPP, and RECO assessments, potentially, can fill the gap in REDD+ carbon accounting.

Credit authorship contribution statement

You-Ren Wang: Conceptualization, Methodology, Software, Formal analysis, Writing - Original Draft, Visualization. **Nina Buchmann**:

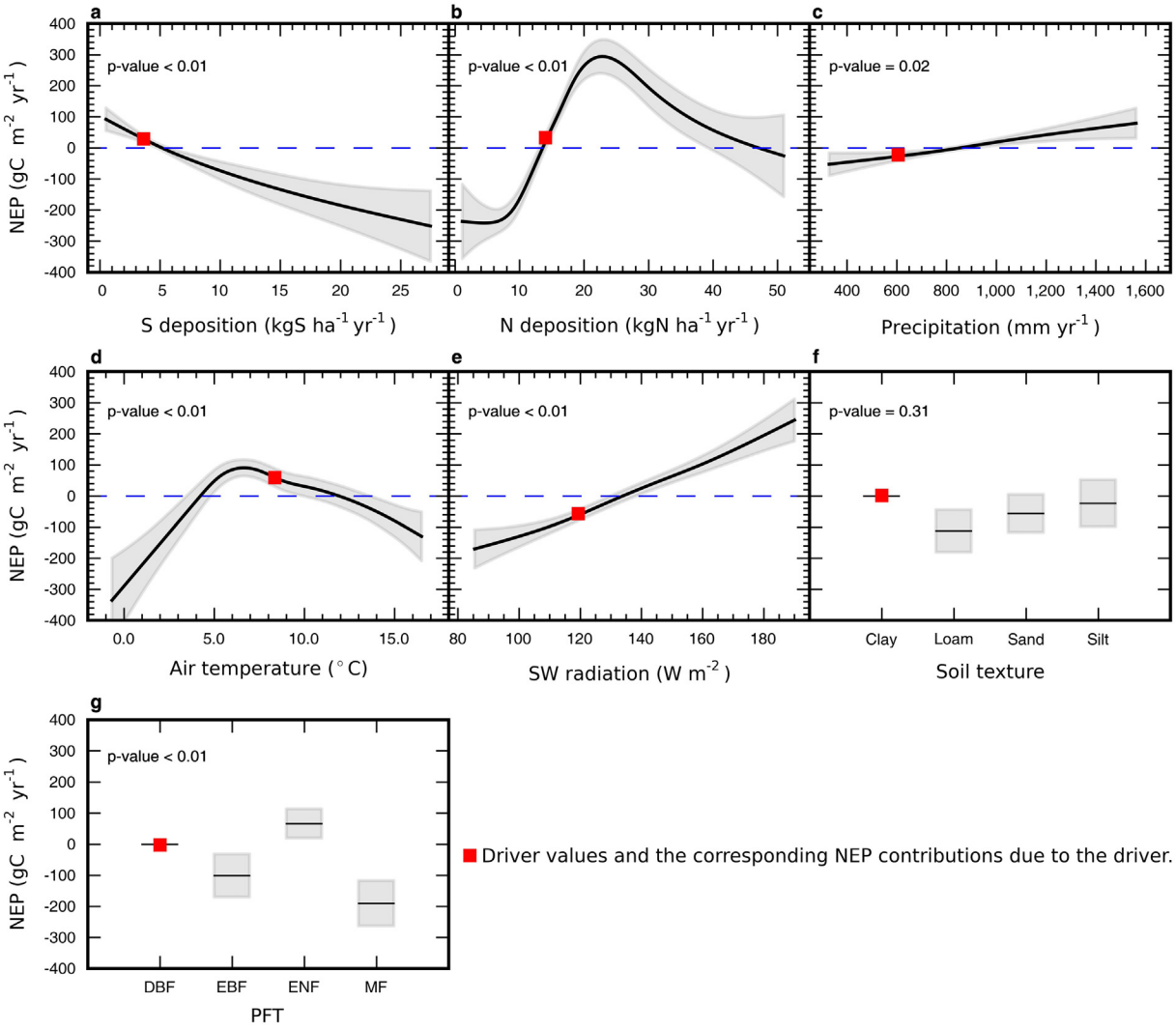

Fig. 6. Illustration of estimating driver contributions to NEP from GAM regression curves for DE-Hai 2008 as an example. For a given driver value, the corresponding NEP contribution can be obtained on the y-axis of the driver panel in Fig. (2).

Conceptualization, Methodology, Writing - Review & Editing. **Dag O. Hessen**: Methodology, Writing - Review & Editing, Funding acquisition. **Frode Stordal**: Methodology, Writing - Review & Editing. **Jan Willem Erisman**: Methodology, Writing - Review & Editing. **Ane Victoria Vollsnes**: Methodology, Writing - Review & Editing. **Tom Andersen**: Methodology, Writing -

Table 3
Estimated driver contributions to NEP from GAM regression curves for CH-Lae 2010, DE-Hai 2008, FR-Pue 2002, and IT-SRo 2007, as example site-years for each of the four PFTs in this study.

		Baseline ($gC\ m^{-2}\ yr^{-1}$)	S dep. ($kgS\ ha^{-1}\ yr^{-1}$)	N. dep. ($kgN\ ha^{-1}\ yr^{-1}$)	Precip. ($mm\ yr^{-1}$)	Temp. (°C)	SW rad. ($W\ m^{-2}$)	Soil	PFT	Modelled NEP ($gC\ m^{-2}\ yr^{-1}$)	Actual NEP ($gC\ m^{-2}\ yr^{-1}$)	Modelled–actual ($gC\ m^{-2}\ yr^{-1}$)
CH-Lae	Driver data		3.9	24.5	1234.8	6.8	132.1	Loam	MF			
2010	Modelled partial NEP ($gC\ m^{-2}\ yr^{-1}$)	478.0	23.3	285.9	45.6	90.2	−7.8	−112.2	−190.1	613.0	624.4	−11.4
DE-Hai	Driver data		3.9	14.8	612.3	8.7	119.7	Clay	DBF			
2008	Modelled partial NEP ($gC\ m^{-2}\ yr^{-1}$)	478.0	24.5	54.9	−26.6	52.3	−60.6	0.0	0.0	522.5	533.5	−11.0
FR-Pue	Driver data		6.7	11.6	1165.8	13.8	161.8	Loam	EBF			
2002	Modelled partial NEP ($gC\ m^{-2}\ yr^{-1}$)	478.0	−26.1	−94.9	38.0	−45.0	110.5	−112.2	−100.6	247.8	258.0	−10.1
IT-SRo	Driver data		6.59	12.65	571.2	15.1	180.9	Sand	ENF			
2007	Modelled partial NEP ($gC\ m^{-2}\ yr^{-1}$)	478.0	−24.1	−44.3	−30.6	−82.7	199.1	−56.0	66.7	506.1	496.9	9.2

Review & Editing. **Han Dolman**: Conceptualization, Methodology, Writing - Review & Editing, Funding acquisition.

Declaration of competing interest

The authors declare that they have no known competing financial interests or personal relationships that could have appeared to influence the work reported in this paper.

Acknowledgments

This work was supported by EU-FP7 projects GHG-Europe (Grant agreement no. 244122) and GEOCARBON (Grant agreement no. 283080). The FLUXNET2015 eddy covariance data used were acquired from and shared by the FLUXNET community, which includes these networks: AmeriFlux, AfriFlux, AsiaFlux, CarboAfrica, CarboEuropeIP, CarboItaly, CarboMont, ChinaFlux, Fluxnet-Canada, GreenGrass, ICOS RI, ICOS-CH, KoFlux, LBA, NECC, OzFlux-TERN, Swiss FluxNet, TCOS-Siberia, and USCCC. The FLUXNET community utilized the ERA-Interim reanalysis data provided by ECMWF and processed by LSCE. The FLUXNET eddy covariance data processing and harmonization were carried out by the European Fluxes Database Cluster, AmeriFlux Management Project, and Fluxdata project of FLUXNET, with the support of CDIAC and ICOS Ecosystem Thematic Center, and the OzFlux, ChinaFlux and AsiaFlux offices. H.D. acknowledges support from the Netherlands Earth System Science Centre (grant no. 024.002.001).

Appendix A. Supplementary data

Supplementary data to this article can be found online at https://doi.org/10.1016/j.scitotenv.2022.156326.

References

Aherne, J., Posch, M., 2013. Impacts of nitrogen and Sulphur deposition on forest ecosystem services in Canada. Curr. Opin. Environ. Sustain. 5, 108–115.
Anderegg, W.R., Martinez-Vilalta, J., Cailleret, M., Camarero, J.J., Ewers, B.E., Galbraith, D., et al., 2016. When a tree dies in the forest: scaling climate-driven tree mortality to ecosystem water and carbon fluxes. Ecosystems 19, 1133–1147.
Baldocchi, D., Falge, E., Gu, L., Olson, R., Hollinger, D., Running, S., et al., 2001. FLUXNET: a new tool to study the temporal and spatial variability of ecosystem-scale carbon dioxide, water vapor, and energy flux densities. Bull. Am. Meteorol. Soc. 82, 2415–2434.
Binkley, D., Högberg, P., 2016. Tamm review: revisiting the influence of nitrogen deposition on swedish forests. For. Ecol. Manag. 368, 222–239.
Blujdea, V.N., Sikkema, R., Dutca, I., Nabuurs, G.-J., 2021. Two large-scale forest scenario modelling approaches for reporting CO2 removal: a comparison for the Romanian forests. Carbon Balance Manage. 16, 1–17.
Bobbink, R., Hettelingh, J., 2011. Review and Revision of Empirical Critical Loads and Dose-response Relationships: Proceedings of an Expert Workshop, Noordwijkerhout, 23-25 June 2010: Rijksinstituut voor Volksgezondheid en Milieu RIVM.
Buja, A., Hastie, T., Tibshirani, R., 1989. Linear smoothers and additive models. Ann. Stat. 453–510.
Chien, S.H., Gearhart, M.M., Collamer, D.J., 2008. The effect of different ammonical nitrogen sources on soil acidification. Soil Sci. 173, 544–551.
Ciais, P., Reichstein, M., Viovy, N., Granier, A., Ogée, J., Allard, V., et al., 2005. Europe-wide reduction in primary productivity caused by the heat and drought in 2003. Nature 437, 529–533.
Ciais, P., Schelhaas, M.-J., Zaehle, S., Piao, S., Cescatti, A., Liski, J., et al., 2008. Carbon accumulation in European forests. Nat. Geosci. 1, 425–429.
Ciais, P., Tan, J., Wang, X., Roedenbeck, C., Chevallier, F., Piao, S.-L., et al., 2019. Five decades of northern land carbon uptake revealed by the interhemispheric CO2 gradient. Nature 568, 221.
Ciais, P., Yao, Y., Gasser, T., Baccini, A., Wang, Y., Lauerwald, R., et al., 2021. Empirical estimates of regional carbon budgets imply reduced global soil heterotrophic respiration. Natl. Sci. Rev. 8, nwaa145.
De Vries, W., Breeuwsma, A., 1987. The relation between soil acidification and element cycling. Water Air Soil Pollut. 35, 293–310.
DeHayes, D.H., Schaberg, P.G., Hawley, G.J., Strimbeck, G.R., 1999. Acid rain impacts on calcium nutrition and forest health alteration of membrane-associated calcium leads to membrane destabilization and foliar injury in red spruce. Bioscience 49, 789–800.
Dietze, M.C., Moorcroft, P.R., 2011. Tree mortality in the eastern and central U nited S tates: patterns and drivers. Glob. Chang. Biol. 17, 3312–3326.
Dilustro, J.J., Collins, B., Duncan, L., Crawford, C., 2005. Moisture and soil texture effects on soil CO2 efflux components in southeastern mixed pine forests. For. Ecol. Manag. 204, 87–97.
Dise, N., Ashmore, M., Belyazid, S., Bleeker, A., Bobbink, R., De Vries, W., 2011. Nitrogen as a threat to European terrestrial biodiversity. In: Sutton, M., Howard, C., Erisman, J., Billen, G., Bleeker, A., Grennfelt, P. (Eds.), The European Nitrogen Assessment: Sources, Effects and Policy Perspectives. Cambridge University Press, Cambridge, pp. 463–494 https://doi.org/10.1017/CBO9780511976988.023.
Durand, M., Murchie, E.H., Lindfors, A.V., Urban, O., Aphalo, P.J., Robson, T.M., 2021. Diffuse solar radiation and canopy photosynthesis in a changing environment. Agric. For. Meteorol. 311, 108684.
Erisman, J., Bleeker, A., Galloway, J., Sutton, M., 2007. Reduced nitrogen in ecology and the environment. Environ. Pollut. 150, 140–149.
Fagerli, H., Tsyro, S., Jonson, J., Nyíri, Á., Gauss, M., Simpson, D., 2019. Transboundary particulate matter, photo-oxidants, acidifying and eutrophying components. EMEP status report 1/2019. https://emep.int/publ/reports/2019/EMEP_Status_Report_1_2019.pdf.
Flechard, C.R., Ibrom, A., Skiba, U.M., de Vries, W., Van Oijen, M., Cameron, D.R., et al., 2020a. Carbon-nitrogen interactions in european forests and semi-natural vegetation-part 1: fluxes and budgets of carbon, nitrogen and greenhouse gases from ecosystem monitoring and modelling. Biogeosciences 1583–1620.
Flechard, C.R., Van Oijen, M., Cameron, D.R., de Vries, W., Ibrom, A., Buchmann, N., et al., 2020b. Carbon-nitrogen interactions in european forests and semi-natural vegetation-part 2: untangling climatic, edaphic, management and nitrogen deposition effects on carbon sequestration potentials. Biogeosciences 17, 1621–1654.
FLUXNET, Fluxdata database. https://fluxnet.org/. (Accessed 24 April 2020).
Forde, B.G., Clarkson, D.T., 1999. Nitrate and ammonium nutrition of plants: physiological and molecular perspectives. Adv. Bot. Res. 30, 1–90.
Fowler, D., 1992. Effects of acidic pollutants on terrestrial ecosystems. In: Radojevic, M., Harrison, R.M. (Eds.), Atmospheric Acidity: Sources, Consequences and Abatement. Elsevier, Amsterdam, pp. 341–361.
Fowler, D., Pilegaard, K., Sutton, M., Ambus, P., Raivonen, M., Duyzer, J., et al., 2009. Atmospheric composition change: ecosystems–atmosphere interactions. Atmos. Environ. 43, 5193–5267.
Friedlingstein, P., O'sullivan, M., Jones, M.W., Andrew, R.M., Hauck, J., Olsen, A., et al., 2020. Global carbon budget 2020. Earth Syst. Sci. Data 12, 3269–3340.
Fry, B.P., 2011. Community forest monitoring in REDD+: the 'M'in MRV? Environ. Sci. Pol. 14, 181–187.
Galloway, J., 1995. Acid deposition: perspectives in time and space. Water Air Soil Pollut. 85, 15–24.
Gauss, M., Tsyro, S., Benedictow, A., Fagerli, H., 2019. EMEP/MSC-W model performance for acidifying and eutrophying components, photo-oxidants and particulate matter in 2017. Supplementary material to EMEP status report 1/2019. Retrieved: https://emep.int/mscw/mscw_publications.html.
Gholz, H., Ewel, K., Teskey, R., 1990. Water and forest productivity. For. Ecol. Manag. 30, 1–18.
Grassi, G., House, J., Kurz, W.A., Cescatti, A., Houghton, R.A., Peters, G.P., et al., 2018. Reconciling global-model estimates and country reporting of anthropogenic forest CO2 sinks. Nat. Clim. Chang. 8, 914–920.
Green, J., Berry, J., Ciais, P., Zhang, Y., Gentine, P., 2020. Amazon rainforest photosynthesis increases in response to atmospheric dryness. Sci. Adv. 6, eabb7232.
Gupta, A., Lövbrand, E., Turnhout, E., Vijge, M.J., 2012. In pursuit of carbon accountability: the politics of REDD+ measuring, reporting and verification systems. Curr. Opin. Environ. Sustain. 4, 726–731.
Harrison, R.M., 2017. In: Hester, R.E., Harrison, R.M. (Eds.), Coal in the 21st Century: Energy Needs, Chemicals and Environmental Controls. Royal Society of Chemistry, United Kingdom 224 pp.
Hastie, T.J., Tibshirani, R.J., 1990. Generalized Additive Models. 1st ed. Routledge https://doi.org/10.1201/9780203753781 352 pp.
Hettelingh, J., Posch, M., Slootweg, J., 2017. European Critical Loads: Database, Biodiversity and Ecosystems at Risk: CCE Final Report 2017.
Jacoby, W.G., 2000. Loess: a nonparametric, graphical tool for depicting relationships between variables. Elect. Stud. 19, 577–613.
Johnson, D.W., 1984. Sulfur cycling in forests. Biogeochemistry 1, 29–43.
Johnston, J.D., Dunn, C.J., Vernon, M.J., 2019. Tree traits influence response to fire severity in the western Oregon cascades, USA. For. Ecol. Manag. 433, 690–698.
Joos, F., Prentice, I.C., Sitch, S., Meyer, R., Hooss, G., Plattner, G.K., et al., 2001. Global warming feedbacks on terrestrial carbon uptake under the intergovernmental panel on climate change (IPCC) emission scenarios. Glob. Biogeochem. Cycles 15, 891–907.
Lindroth, A., Grelle, A., Morén, A.S., 1998. Long-term measurements of boreal forest carbon balance reveal large temperature sensitivity. Glob. Chang. Biol. 4, 443–450.
Luyssaert, S., Schulze, E.-D., Börner, A., Knohl, A., Hessenmöller, D., Law, B.E., et al., 2008. Old-growth forests as global carbon sinks. Nature 455, 213.
Ma, L., Hurtt, G., Tang, H., Lamb, R., Campbell, E., Dubayah, R., et al., 2021. High-resolution forest carbon modelling for climate mitigation planning over the RGGI region, USA. Environ. Res. Lett. 16, 045014.
Magnani, F., Mencuccini, M., Borghetti, M., Berbigier, P., Berninger, F., Delzon, S., et al., 2007. The human footprint in the carbon cycle of temperate and boreal forests. Nature 447, 849.
Maniatis, D., Mollicone, D., 2010. Options for sampling and stratification for national forest inventories to implement REDD+ under the UNFCCC. Carbon Balance Manage. 5, 1–14.
MET, EMEP MSC-W modelled air concentrations and depositions. https://www.emep.int/mscw/mscw_moddata.html. (Accessed 20 November 2019).
Mitchell, A.L., Rosenqvist, A., Mora, B., 2017. Current remote sensing approaches to monitoring forest degradation in support of countries measurement, reporting and verification (MRV) systems for REDD+. Carbon Balance Manage. 12, 1–22.
Nilsson, J., 1988. Critical loads for Sulphur and nitrogen. Air Pollut. Ecosyst. 85–91.
Ochieng, R., Visseren-Hamakers, I., Brockhaus, M., Kowler, L., Herold, M., Arts, B., 2016. Historical development of institutional arrangements for forest monitoring and REDD+ MRV in Peru: discursive-institutionalist perspectives. Forest Policy Econ. 71, 52–59.

Papale, D., Black, T.A., Carvalhais, N., Cescatti, A., Chen, J., Jung, M., et al., 2015. Effect of spatial sampling from european flux towers for estimating carbon and water fluxes with artificial neural networks. J. Geophys. Res. Biogeosci. 120, 1941–1957.

Papale, D., Reichstein, M., Aubinet, M., Canfora, E., Bernhofer, C., Kutsch, W., et al., 2006. Towards a standardized processing of net ecosystem exchange measured with eddy covariance technique: algorithms and uncertainty estimation. Biogeosciences 3, 571–583.

Pastorello, G., Papale, D., Chu, H., Trotta, C., Agarwal, D., Canfora, E., et al., 2017. A new data set to keep a sharper eye on land-air exchanges. EOS Trans. Am. Geophys. Union 98.

Pastorello, G., Trotta, C., Canfora, E., Chu, H., Christianson, D., Cheah, Y.-W., et al., 2020. The FLUXNET2015 dataset and the ONEFlux processing pipeline for eddy covariance data. Sci. Data 7, 1–27.

Pregitzer, K.S., Burton, A.J., Zak, D.R., Talhelm, A.F., 2008. Simulated chronic nitrogen deposition increases carbon storage in northern temperate forests. Glob. Chang. Biol. 14, 142–153.

Reay, D.S., Dentener, F., Smith, P., Grace, J., Feely, R.A., 2008. Global nitrogen deposition and carbon sinks. Nat. Geosci. 1, 430.

Reichstein, M., Carvalhais, N., 2019. Aspects of forest biomass in the earth system: its role and major unknowns. Surv. Geophys. 40, 693–707.

Reichstein, M., Falge, E., Baldocchi, D., Papale, D., Aubinet, M., Berbigier, P., et al., 2005. On the separation of net ecosystem exchange into assimilation and ecosystem respiration: review and improved algorithm. Glob. Chang. Biol. 11, 1424–1439.

Ruimy, A., Jarvis, P., Baldocchi, D., Saugier, B., 1995. CO2 fluxes over plant canopies and solar radiation: a review. Adv. Ecol. Res. 26, 1–68.

Schulze, E.-D., 2006. Biological control of the terrestrial carbon sink. Biogeosciences 3, 147–166.

Schulze, E.-D., Beck, E., Buchmann, N., Clemens, S., Müller-Hohenstein, K., Scherer-Lorenzen, M., 2019. Plant Ecology. Springer, Berlin, Heidelberg https://doi.org/10.1007/978-3-662-56233-8.

Schulze, E.-D., Lange, O.L., Oren, R., 1989. In: Schulze, E.-D., Lange, O.L., Oren, R. (Eds.), Forest Decline and Air Pollution: A Study of Spruce (Picea abies) on Acid Soils. Springer-Verlag.

Schwalm, C.R., Williams, C.A., Schaefer, K., Arneth, A., Bonal, D., Buchmann, N., et al., 2010. Assimilation exceeds respiration sensitivity to drought: a FLUXNET synthesis. Glob. Chang. Biol. 16, 657–670.

Simpson, D., Benedictow, A., Berge, H., Bergström, R., Emberson, L.D., Fagerli, H., et al., 2012. The EMEP MSC-W chemical transport model–technical description. Atmos. Chem. Phys. 12, 7825–7865.

Simpson, D., Butterbach-Bahl, K., Fagerli, H., Kesik, M., Skiba, U., Tang, S., 2006. Deposition and emissions of reactive nitrogen over european forests: a modelling study. Atmos. Environ. 40, 5712–5726.

Sirro, L., Häme, T., Rauste, Y., Kilpi, J., Hämäläinen, J., Gunia, K., et al., 2018. Potential of different optical and SAR data in forest and land cover classification to support REDD+ MRV. Remote Sens. 10, 942.

Stevens, C.J., Dise, N.B., Gowing, D.J., 2009. Regional trends in soil acidification and exchangeable metal concentrations in relation to acid deposition rates. Environ. Pollut. 157, 313–319.

Thomas, R.Q., Canham, C.D., Weathers, K.C., Goodale, C.L., 2010. Increased tree carbon storage in response to nitrogen deposition in the US. Nat. Geosci. 3, 13.

UNFCCC, 2015. Paris agreement. Report of the Conference of the Parties to the United Nations Framework Convention on Climate Change (21st Session, 2015: Paris). 4. HeinOnline, p. 2017 Retrived December 2021.

UNFCCC, REDD+ framework. https://unfccc.int/topics/land-use/workstreams/reddplus. (Accessed 24 February 2022).

Vargas, R., Paz, F., de Jong, B., 2013. Quantification of forest degradation and belowground carbon dynamics: ongoing challenges for monitoring, reporting and verification activities for REDD+. Carbon Manage. 4, 579–582.

von Buttlar, J., Zscheischler, J., Rammig, A., Sippel, S., Reichstein, M., Knohl, A., et al., 2018. Impacts of droughts and extreme-temperature events on gross primary production and ecosystem respiration: a systematic assessment across ecosystems and climate zones. Biogeosciences 15, 1293–1318. https://doi.org/10.5194/bg-15-1293-2018.

Welp, L., Randerson, J., Liu, H., 2007. The sensitivity of carbon fluxes to spring warming and summer drought depends on plant functional type in boreal forest ecosystems. Agric. For. Meteorol. 147, 172–185.

Wood, S., 2022a. mgcv: mixed GAM computation vehicle with automatic smoothness estimation. https://cran.r-project.org/web/packages/mgcv/index.html.

Wood, S., 2022b. Package 'mgcv'. https://cran.r-project.org/web/packages/mgcv/mgcv.pdf.

Wood, S.N., 2004. Stable and efficient multiple smoothing parameter estimation for generalized additive models. J. Am. Stat. Assoc. 99, 673–686.

Wood, S.N., 2017. Generalized Additive Models: An Introduction With R. CRC press.

Yee, T.W., Mitchell, N.D., 1991. Generalized additive models in plant ecology. J. Veg. Sci. 2, 587–602.